JOURNAL OF OPTOELECTRONICS AND ADVANCED MATERIALS Vol. 8, No. 3, June 2006, p. 1234 - 1237

Preparation and structural characterization of nickel/ alumina nano-particles composite coatings

C. GHEORGHIES, G. CARAC, I. V. STASI
Faculty of Sciences“Dunarea de Jos” University of Galati, Galati R-6200, Romania

The addition of alumina nano-particles into nickel plating bath leads to significantly changes for the surface morphology and for the preferred crystallographic orientation of the composite coatings deposited on Inconel substrates. The typical morphology for nickel deposits from an additive-free bath is pyramidal; however the addition of alumina particles in concentrations between 5 g/l and 10 g/l changes this morphology to hemispherical. The preferred growth direction was also influenced by alumina nano-particles. Therefore, the preferred growth process of the nickel matrix in crystallographic directions <111>, <200> and <220> is strongly influenced at a concentration of 5 g/l, while at a concentration of 10 g/l the influence is very small. When alumina nano-particles were absent from the electroplating bath the growth took place preferentially on (200) oriented planes. However, alumina in small amount acts towards improving the growth of grains of this orientation. Nano-particles of alumina influence the level of the first order tensions determined by the X-ray diffraction technique by means of the $sin^2 \psi$ method. The concentration of 10 g/l leads to a bigger level of the first order tension in the matrix of nickel of electrodeposited composite, as compared to the concentration of 5 g/l.

(Received February 20, 2006; accepted May 18, 2006)

Keywords: Co-deposition, Nickel, Nano- alumina particles, Composites, Structure

1. Introduction

Composite metal/non-metal electroplated coatings have a wide variety of practical applications. Particles of oxides [1,2], carbides [3,4] and nitride [5] having micrometer and sub-micrometer dimensions can be deposited together with various metal electroplates such as Co, Cu and Ni. Moreover, addition of metal-inorganic particles composite can lead obtaining special properties of coatings such as good hardness and wear corrosion resistance, and metal-organic particles can determine new characteristics such as self-lubricating coatings [6]. In the last 15 years [7-9], electrodeposited composite coating technology, in which particles are co-deposited with a metal by electrodeposition, has progressed greatly. The mechanisms associated with the composite plating process have been investigated and some models have proposed [10], but little researches have been performed to investigate the effect of introducing non-metallic particles on the electroplate growth morphology. This is not necessary since the correlation of property data with non-metallic particles may be incorrect due to synergetic effects arising from a modified metal microstructure [11].

The grain structure of pure nickel coatings has been studied in numerous works and results indicate that, following the nucleation stage, preferential growth occurs on favourably oriented grains. The growth mechanism involves deposition on pyramidal grain surfaces resulting in surface roughening and loss of substrate surface character. Preferential growth modes in electrocrystallized nickel arise due to the inhibition of other growth modes. The most common inhibitors affecting the growth process are hydrogen gas, absorbed hydrogen atoms or nickel hydroxide at the electrolyte-substrate surface. Thus, in [18] is shown that the preferred growth direction for nickel is the <100> direction, and that the adsorbed hydrogen inhibits growth in all crystallographic directions except <110>, gaseous hydrogen involves the preferred growth <210> direction, while nickel hydroxide facilitates <211> preferred growth. Moreover, the pH, the current density, the local concentrations and various electrolyte additions lead to achievement of preferred or random deposit growth textures.

During electroplating metal-oxide composite coatings, it is necessary to investigate the effects of adding the metal oxide to the electrolyte pH. If the pH of the electrolyte rises greatly, e.g. over 5, excessive hydroxide precipitation can occur and the coatings are of poor quality. A high value of pH leads to appearance of hydrated oxide cations that occur to an uncontrolled development of the coating, also. The present paper investigates the effects of alumina nano-particles in the electrolyte bath, and of current density on the growth textures and surface morphologies of nickel electrodeposited that constitutes a nanocomposite material.

2. Experimental

The electroplating cell used for the co-deposition experiments in Fig. 1 is shown. The bath was manufactured form Jena glass and has a capacity of 500 cm^3. A water jacket for controlled heating surrounds it. The stirrer device used was a porous bottom plate agitator that consists of a perforate plate finally ensuring the presence of alumina nano-particles in electrolyte. The anode made of nickel is of square form with dimension of 50×50×3 mm, and the cathode is made of Inconel and placed at a distance of 50 mm. The chemical composition of Inconel is presented in Table 1.

Table 1.

Element	Ni	Cr	Mo	Fe	Nb	Co	Mn	Si	Ti	Al	C
(%)	58.0	21.0	8.0	5.0	3.6	1.0	0.5	0.5	0.3	0.4	0.1

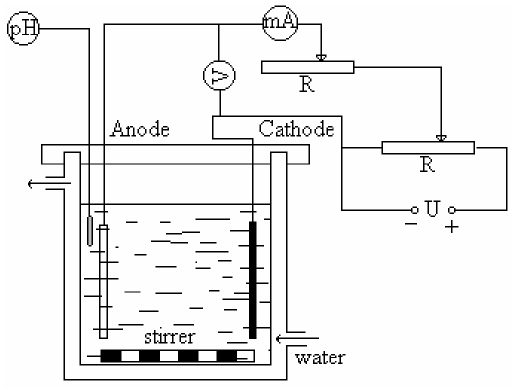

Fig. 1. Electroplating cell and electrode arrangement.

The bath used for the electroplating was a nickel bath, consisting of 0.90M $NiSO_4 \cdot 6H_2O$, 0.20M $NiCl_2 \cdot 6H_2O$, 0.30M H_3BO_3 and 0.4g/l sodium dodecylsulphate [$CH_3(CH_2)_{11}OSO_3Na$]. Alumina was been delivered by Degusa Company and its concentration in the bath varied from 0 to 20g/L. The size of the alumina particles was of 20nm and they were kept in suspension by means of a magnetic stirrer. The stirring rate of the plate agitator is of 700 rpm. During the electroplating process, the operating temperature was of 40 ^{o}C. The electrolyte pH value was in the range of 4.2-4.4 by addition of hydrochloric acid. The current density was of 2A dm^{-2} and the deposition time up to 90 min.

The main tools used for the surface characterisation were scanning electron microscopy (SEM) equipped with a microprobe (EDXS) along with X-ray diffractometer (XRD). The OLYMPUS PM3 microscope allows for morphological observations of microstructure. The XRD used was a Philips Xpert, and the determination of the crystal structure present in the coating, and the effect that alumina has on the coating surface have been carried out. Nickel having a face centred cubic structure, upon analysis by XRD shows that only certain planes common to the nickel system are expected, and these in Table 2 are presented.

Table 2.

(hkl)	2θ (^{o})	I (a.u.)
111	44.51	100
200	51.85	42
220	76.37	21
311	92.94	20

3. Results and discussion

Fig. 2 compares two cross view microscopic images, obtained at two different magnifications for the same electrodeposited layer of nickel having 20% alumina nanoparticles concentration. In the first image alumina particles are not distinctively observed, while in the second image some agglomeration of alumina particle can be viewed in the electrodeposited layer.

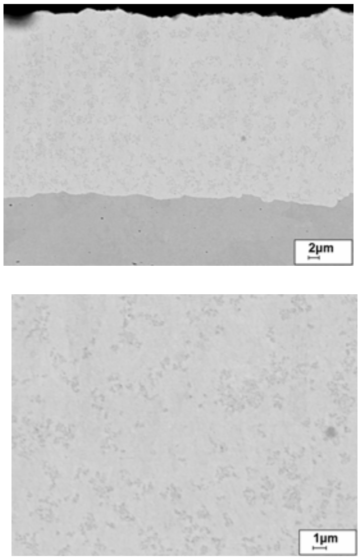

Fig. 2. Cross views of the electrodeposited film of nickel / alumina nanoparticles

Fig. 3 presents a general view of the cross section of the prepared composite material when the alumina nanoparticles composition is of 10g/l, therefore showing different thicknesses of the electrodeposited layer. Fig. 4 shows how alumina nanoparticles concentration influences the roughness of the electrodeposited coating.

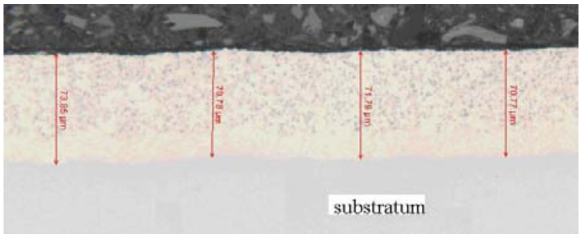

Fig. 3. General view of electrodeposited film of nickel / alumina nanoparticles.

The deposits of pure Ni and Ni/Al_2O_3 composite coatings present a variable layers thickness. The thickness depends on the current density, the deposition time, and all the other variables of the electrocodeposition process. Additionally, the concentration the dispersed particles in the electrolyte has an effect on the thickness. During the deposition process of 90 minutes a thickness between 40-75 μm was founded, which can be shown in Fig. 5. The thickness obtained at low particle concentration (5 g/l) in the bath is about 100 % higher than in the case of pure nickel deposition. This effect can be due to the surface area effect. In the case of higher particles concentrations, the layer thickness decreases. This fact can be explained by the growth of the agglomerating particles, in the layers that became bigger in the case of higher amounts of particles.

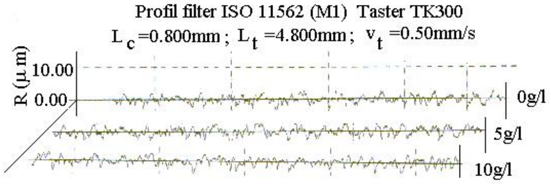

Fig. 4. Influence of the alumina concentration on micro geometry of electrodeposited film.

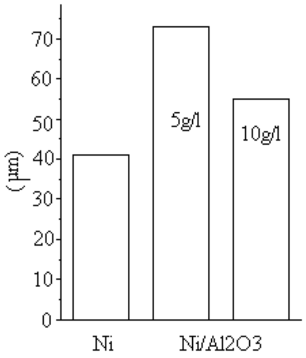

Fig. 5.Thickness of Ni/Al_2O_3 composite coatings

In Fig. 6 two SEM images of electrodeposition are displayed for alumina nanoparticles concentrations of 5 g/l, and 10 g/l, respectively.

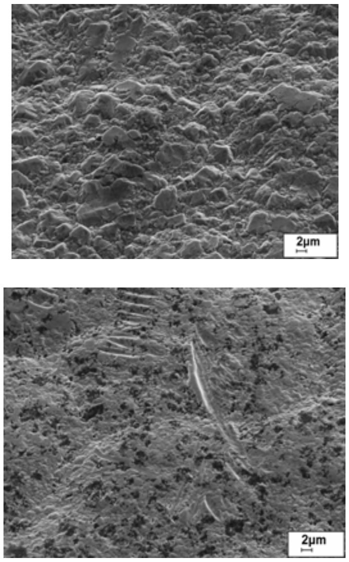

Fig. 6. SEM images of nickel electrodeposition for 5 g/l (top) and 10 g/l (bottom) alumina concentration.

As alumina was added to the electrolyte in increasing concentrations, a general refinement in the grain structure on the surface is observed. With addition of 5 g/l of alumina, the average size of the pyramids on the surface is clearly reduced. There is also a reduction in the surface grain size to micrometer and sub micrometer grains. These results show that the surface morphology is greatly refined by the presence of alumina in the bath for the coatings deposited at 2 A.dm^{-2}. The other images show that in the case of a bath containing 0 and 1 g/l alumina no significant difference in surface grain size are observed. The grain size of nickel matrix ranges from 2.0 to 4.5 μm. For higher alumina concentration a reduction of grain size, to between 1 and 3μm, was noticed. The large pyramidal grains that were presented at low concentration disappeared with the higher alumina quantity. Generally, the SEM images precisely show that the morphology of surface is refined by alumina additions, for current density taken at 2 A.dm^{-2}.

The chemical analysis of electrodeposited layer by EDXS method has been estimated, and in Fig. 7 a typical spectrum showing the chemical constitution is presented.

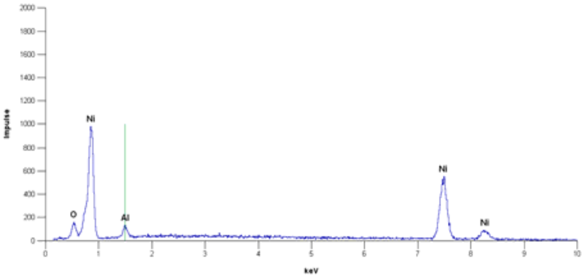

Fig. 7. EDXS spectrum of electrodeposited film.

In Fig. 8 an X-ray pattern from an electrodeposited film of nickel having a concentration of 10% alumina nanoparticles is presented.

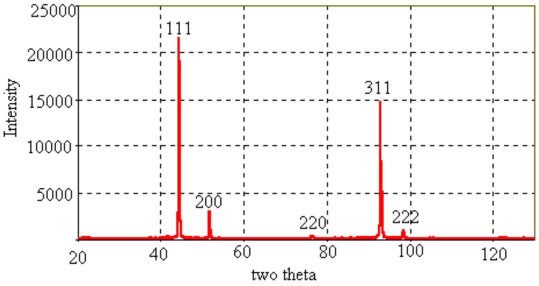

Fig. 8. X-ray diffraction spectrum of electrodeposited nickel film with 10% alumina nanoparticles.

According to data from Table 2 only the characteristic peaks of nickel can be noticed. This is probably due to the fact that the concentration of alumina in solution is small and in X-ray diffraction spectrum the characteristic peaks of alumina didn't appear. The concentration of alumina influences the position of some nickel layer in the x-ray diffraction spectrum. It is seen that for the Inconel substrate the relative intensity of the (111) reflection is much greater than the relative intensity of the other reflections like (200, (220), and (311) and, thus, the Inconel substrate exhibits a (111) <111> preferred orientation. Other x-ray patterns showed that as the alumina loading increases then the preferred orientation factor increases too for small current densities, up to 10 mA/cm^2, but this has little effect at higher current densities. For higher alumina loading, the intensities of the (111) and (311) peaks predominate significantly. Thus it can be said that the growth mode of the nickel deposit in the presence of alumina changes from <100> growth mode.

In Fig. 9 the dependence of mosaic block dimension of deposited nickel versus interplanar distance for three different concentrations of alumina is presented. The displayed curves show that there is a general tendency towards increasing the mosaic block dimension along with the interplanar distance. The presented data have a technical importance showing the possibility to adjust the dimension of nickel particle by means of concentrations of nanoparticles alumina.

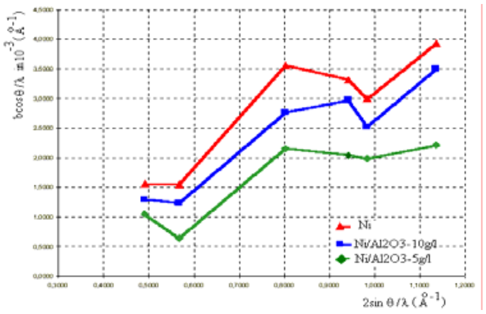

Fig. 9. Dependence of the mosaic block dimension versus the interplanar distance.

In Fig. 10 are shown certain extrapolation curves concerning the determination of lattice parameter of nickel electrodeposited for three concentrations of alumina. It can be seen the strong influence of the lattice parameter of alumina presence and a small influence of the alumina concentration.

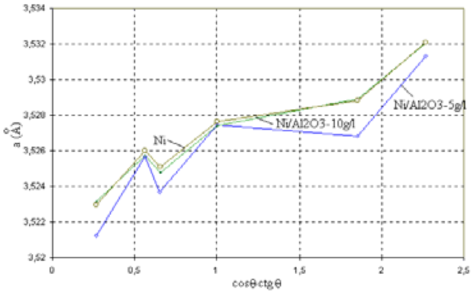

Fig. 10. Extrapolation curves for determining the lattice parameter, a, for nickel electrodeposited.

In Fig. 11 the dependence of the X-ray diffraction intensity versus alumina concentration for different incident angles of X-rays in case of the (220) crystallographic plane is presented. These curves offer information on the texture degree of the electrodeposited nickel in the presence of alumina nanoparticles. It can be seen the influence of the alumina concentration on the orientation degree of the (220) crystalline planes of electrodeposited nickel in the deposited layer. Similar influences of alumina concentration on texture degree of electrodeposited nickel for other crystalline planes are pointed out.

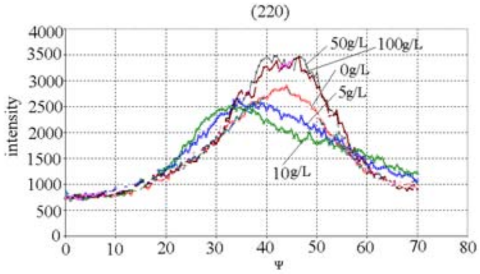

Fig. 11. Dependence of the X-ray diffraction intensity versus the incidence angle of X-ray beam

4. Conclusions

The electro-codeposition of nickel and alumina nanoparticles was investigated. This study was made to evaluate the influences of nanoparticles addition on some morphologic and structure characteristics. The nanoparticles appear agglomerated in the layers of a nickel matrix without having a crystalline structure. Additions of alumina particles with a particle size of 20 nm of 5 g/l and 10 g/l into nickel plating bath change the preferred growth direction of the electrodeposited nickel from <100> to <111>. This change is not induced by the epitaxial effects of substrate, which show a predominant (111) reflection, or by the presence of alumina in the bath. The microstructure of composite coatings is changed in comparison with pure nickel deposits, when alumina was added. The coating surfaces can be produced to be smooth and dense, but also roughness.

Acknowledgement

The authors thank to T. Lempke and S. Steinhäuser from Chemnitz University, Germany, for the support of this work.

References

[1] C White, J. Foster, Trans. Inst. Met. Finish. **59**, 8 (1981).
[2] X. Peng, D. H. Ping, T. F. Li, W. T. Wu, J. Electrochem. Soc. **145**, 389 (1998).
[3] S. H. Yeh, C. C. Wan, J. Appl. Electrochem. **24**, 993 (1994).
[4] K. Foster, B. Cameron, Trans. Inst. Met. Finish. **54**, 178 (1976).
[5] K. Funtani, K. Kurosawa, SAMPE J. **146**, 27 (1994).
[6] E. Pena-Munoz, P. Bercot, A. Grosjean, M. Rezrazi, J. Pagetti, Surf. Coat. Technol. **107**, 85 (1998).
[7] K. Helle, F. Walsh, Trans. Inst. Met. Finish. **75,** 53 (1997).
[8] J. L. Stojak, J. B. Talbot, J. Electrochemical Society **146**, 12 (1999).
[9] J. R. Roos, J. P. Celis, J. Fransaer, C. Buelens, JOM **42**, 60 (1990).
[10] C. Kerr, D. Barker, F. Walsh, J. Archer, Trans. Inst. Met. Finish. **78**, 171 (2000).
[11] A. G. McCormack, M. J. Pomeroy, V. J. Cunnane, J. Electrochem. Soc. **150**, 5 (2003).

---

[*] Corresponding author: cgheorghies@ugal.ro